Proceedings of the 21st ICSMGE, Vienna, Austria, 14 – 19 June 2026. Pistrol, Adam & Schweiger (eds.)
Published by: ÖGG, Austrian Society for Geomechanics, Salzburg, Austria, ISBN 978-3-9503898-4-5
https://doi.org/10.53243/ICSMGE2026-1091

Enhancing Pile Bearing Capacity Prediction for Prebored and Precast PHC Piles Using Advanced AI Models

Seunghwna Seo & Moonkyung Chung
Korea Institute of Civil Engineering and Building Technology, Republic of Korea, seunghwanseo@kict.re.kr

ABSTRACT: Rapid urbanization and concentrated construction in metropolitan areas demand accurate methods for estimating the bearing capacity of pile foundations. This study investigates the use of machine learning (ML) to predict the pile bearing capacity (PBC) of prebored and precast piles (PPP) constructed with pretensioned prestressed high-strength concrete (PHC). A dataset of 217 dynamic load tests was analyzed using three advanced ML models—K-Nearest Neighbor Regression (KNR), Extreme Gradient Boosting (XGB), and Deep Neural Networks (DNN)—for both End of Initial Driving (EOID) and Restrike phases. Among these, the DNN achieved the highest accuracy, with R^2 values of 0.960 (EOID) and 0.915 (Restrike), and exhibited the lowest prediction errors. SHAP-based interpretability analysis identified pile diameter and ram weight as the most influential factors, offering insights into the physical mechanisms underlying PBC. Compared to conventional dynamic driving formulas, which often misestimate capacity due to simplified assumptions about energy transfer and set values, the ML models—particularly DNN—captured complex nonlinear patterns in the geotechnical data with high reliability. The results demonstrate that integrating DNN into pile testing workflows can provide rapid, accurate predictions, enhancing decision-making, reducing project costs and durations, and maintaining safety standards. This study fills a notable gap in the literature on PPPs and establishes a new benchmark for applying AI to geotechnical engineering practice.

KEYWORDS: Pile foundation, pile bearing capacity, prebored and precast pile, machine learning.

1 INTRODUCTION

The rapid growth of urban development has driven advancements in foundation engineering technologies. In metropolitan areas, where environmental impact and construction efficiency are critical, pile foundations are essential for structural stability. Among various types, prebored and precast piles (PPP) fabricated from pre-tensioned pre-stressed high-strength concrete (PHC) have gained popularity for their high compressive strength, durability, and reduced environmental impact (Jung et al., 2017; Kim et al., 2020; Zhou et al., 2020). The PPP method—drilling boreholes, placing precast piles, and grouting the annular space—enhances pile–soil interaction, reduces noise and vibration, and ensures uniform quality through factory-controlled manufacturing (Li and Li, 2023). For PPP, pile bearing capacity (PBC) is evaluated in two stages: the End of Initial Driving (EOID) phase, immediately after installation, and the Restrike phase, after grout curing. These phases reflect time-dependent changes in load transfer capacity due to grout strength gain and setup effects. Conventional methods such as Static Load Testing (SLT) and Dynamic Load Testing (DLT) using Pile Driving Analyzers (PDA) offer practical alternatives for PBC evaluation (Chen et al., 2022; Heins and Grabe, 2020; Kordjazi et al., 2014). Empirical dynamic formulas (Hiley, Danish, Gates) have also been applied (Fragaszy et al., 1986; Lawton et al., 1986; Allin et al., 2015), with recent improvements incorporating time effects (Denes and Kroenert, 2019; Bian et al., 2022; Seo et al., 2023). However, these approaches often oversimplify PPP's complex mechanical interactions and show limited applicability. Machine Learning (ML) has emerged as a powerful tool for modeling complex, non-linear relationships in geotechnical engineering (Hazbeh et al., 2024; Li et al., 2024), yet existing studies largely focus on driven piles. This study addresses that gap by applying K-Nearest Neighbor Regression (KNR), Extreme Gradient Boosting (XGB), and Deep Neural Networks (DNN) to predict PBC at both EOID and Restrike phases using 217 DLT results from domestic PHC PPP. The models are compared against traditional formulas, and SHapley Additive exPlanations (SHAP) are employed to identify key influencing factors, providing a practical and accurate tool for PPP quality control.

2 METHODOLOGY

The overall analysis workflow is shown in Figure. 1. Dynamic load test data for prebored and precast PHC piles were first collected and preprocessed through normalization, outlier removal, and feature engineering. The processed dataset was split into training and testing sets (9:1 ratio), with the training set evaluated using 10-fold cross-validation to ensure generalization and mitigate partitioning bias. Three machine learning models were employed: K-Nearest Neighbors Regression (KNR) for its ability to capture local nonlinear patterns in a simple, interpretable framework; eXtreme Gradient Boosting (XGB) as a robust ensemble method effective in handling complex data while controlling overfitting; and a Deep Neural Network (DNN) capable of modeling highly nonlinear relationships through multi-layer architectures. This combination provided a spectrum of modeling approaches, from simple to complex, for pile bearing capacity prediction. Hyperparameters for each model were optimized based on cross-validation performance metrics. The tuned models were then applied to the test dataset, and their predictions were compared against traditional dynamic driving formulas (Hiley, Danish, Gates) and modified versions incorporating dynamic load test results. To enhance interpretability, SHAP value analysis was conducted, identifying key influencing factors such as pile diameter and ram weight. Finally, the models' applicability was assessed in the context of varying pile characteristics, enabling a comprehensive evaluation that integrates advanced ML techniques with established empirical and energy-based methods for bearing capacity estimation.

3 DATA PREPARATION AND EXPERIMENTAL SETUP

3.1 *Data description*

The dataset consists of 217 dynamic load test (DLT) records for prebored and precast PHC piles. Independent variables range from Diameter to Elapsed time, while bearing capacity in EOID and Restrike are the dependent variables. To reduce multicollinearity, Thickness and Final depth—highly correlated independent variables—were excluded. Although Ram is

correlated with Diameter, it was retained as it, along with Drop height, uniquely represents pile driving energy. The final set of independent variables includes Diameter, Pile length, Drop height (EOID, Restrike), Ram, Set (EOID, Restrike), and Elapsed time, totaling six inputs. Elapsed time was used only for Restrike PBC prediction, as it reflects grout curing, which does not influence EOID capacity. Most piles have diameters under 600 mm, with a few up to 1000 mm. Pile length, Drop height, and Ram values vary, while most Set values are below 3 mm. The mean PBC is 4031.98 kN for EOID and 4784.24 kN for Restrike. Large-diameter piles contribute to higher PBC variability, enabling model training across diverse conditions.

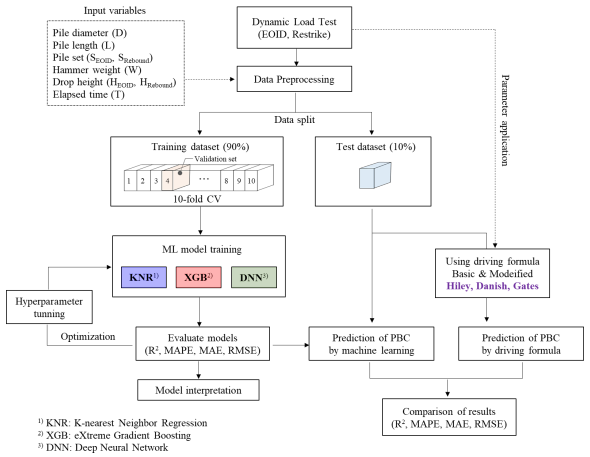

Figure 1. Analytical procedure of developing the pile bearing capacity prediction model

3.2 *Data preprocessing and hyperparameter selection*

The dataset, obtained from dynamic load tests on major construction sites in South Korea, underwent rigorous quality control. Field measurements were cross-verified with site documentation, and only records with a Matching Quality (MQ) score of 2–3 from CAWAP analysis were retained. Outliers were detected using the interquartile range method and either removed or replaced with mean values, and all input variables were normalized to a [0, 1] range using Min–Max scaling to ensure stable learning. To address the limited dataset size, 10-fold cross-validation was employed for robust performance evaluation and to reduce bias caused by data partitioning. Model-specific hyperparameter tuning was performed to achieve an optimal balance between predictive accuracy and overfitting prevention. For the KNR model, the optimal number of neighbors was determined to be k=7 using MSE as the evaluation metric. The XGB model was tuned to use n_estimators=300, learning_rate=0.01, and max_depth=8, which provided the highest R^2 score while maintaining a balance between bias and variance. For the DNN model, a four-layer architecture with 256 nodes per layer, ReLU activation, the Adam optimizer, and a batch size of 10 was selected, as this configuration minimized MSE and avoided overfitting. The final hyperparameter settings for each model are summarized in Table 1, ensuring reproducibility and optimal performance in predicting pile bearing capacity.

Table 1. Control parameter and optimized hyperparameter of KNR, XGB, and DNN

Model	Control parametet
KNR	n_neighbors = 7 Distance Metric = Euclidean Weight Function = Uniform Cross-Validation = 10-fold
XGB	n_estimators = 300 learning_rate = 0.05 max_depth = 8 subsample = 0.8 colsample_bytree = 0.8 lambda = 1 Cross-Validation = 10-fold
DNN	Hidden Layers = 4 Nodes per Layer = 256 Activation = ReLU Optimizer = Adam Learning Rate = 0.001 Batch Size = 10 Epochs = 500 Loss Function = MSE Early Stopping (patience=20) Cross-Validation = 10-fold

3.3 *Performance metric*

Model performance was assessed using four standard regression metrics: R^2, RMSE, MAE, and MAPE. R^2 quantifies the proportion of variance explained by the model, while MAE and RMSE measure the absolute and squared prediction errors, respectively—RMSE being more sensitive to large deviations. MAPE expresses the average percentage error, enabling scale-independent comparison across models. These complementary metrics provide a balanced evaluation of model accuracy and robustness. A summary of the metrics and their formulations is presented in Table 2. Here, y_i represents the actual measured values, and $\hat{y}_i$ denotes the values predicted by the model, and $\bar{y}_i$ represents the mean of the actual measured values across the dataset.

Table 2. Summary of performance metrics

Metric	Formula
R^2	$R^2 = 1 - \frac{\sum_{i=1}^{n}(y_i-\hat{y}_i)^2}{\sum_{i=1}^{n}(y_i-\bar{y}_i)^2}$
RMSE	$RMSE = \sqrt{\frac{1}{n}\sum_{i=1}^{n}(y_i-\hat{y}_i)^2}$
MAE	$MAE = \frac{1}{n}\sum_{i=1}^{n}\lvert y_i-\hat{y}_i\rvert$
MAPE	$MAPE = \sum_{i=1}^{n}\left\lvert\frac{y_i-\hat{y}_i}{y_i}\right\rvert\frac{1}{n}$

4 RESULTS

4.1 *Performance comparison of AI-based prediction models*

Three machine learning models—KNR, XGB, and DNN—were evaluated for predicting the pile bearing capacity (PBC) of prebored and precast PHC piles (PPP) during both the EOID and Restrike phases, using performance metrics calculated on the test datasets (Figure 2). Scatter plots in Figure 2 compare the measured CAPWAP values with model predictions, where points closer to the best-fit line indicate higher predictive accuracy. For the EOID phase, all models captured the overall trend of the measured values; however, prediction accuracy declined for higher PBC values. The DNN achieved the highest test R^2 value (0.960), followed by XGB and KNR. Although KNR attained a near-perfect training R^2 (0.997), it exhibited overfitting, as evidenced by a drop in test R^2 to 0.919 and an increase in MAPE from 0.006 in training to 0.102 in testing. XGB showed better generalization, with a training R^2 of 0.979 and a test R^2 of 0.931, along with a smaller change in MAPE. The DNN, despite a lower training R^2 (0.904), demonstrated the most consistent performance between training and test sets, with minimal differences in RMSE and MAE. For the Restrike phase, model performance generally declined compared to EOID. The DNN again achieved the highest explanatory power (test R^2 = 0.915), although MAPE values indicated that XGB and KNR produced lower average percentage errors. Overfitting tendencies were more pronounced in KNR and

XGB, particularly in the EOID phase. Overall, while all models exhibited strong predictive capabilities, the DNN demonstrated the best generalization across both phases, making it a promising candidate for practical PBC prediction in PPP, particularly when balancing accuracy and robustness.

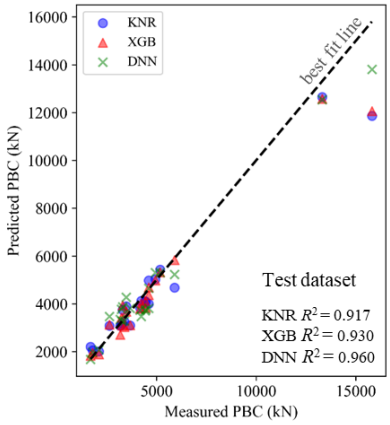

(a) EOID phase

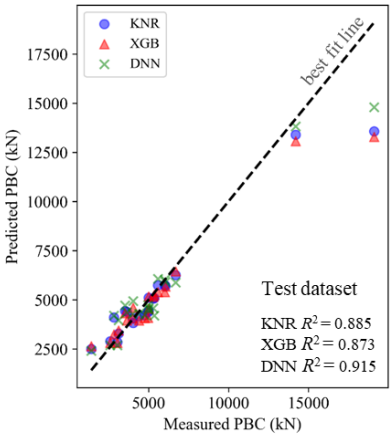

(b) Restrike phase

Figure 2. Prediction results of AI models with driving phase for test dataset

4.2 *Comparison of prediction results of AI models and dynamic driving formulas*

Figure 3 compares the EOID and Restrike PBC predictions from AI models with those from traditional and modified dynamic driving formulas. For EOID, AI models closely follow the best-fit line, indicating high accuracy, whereas the Hiley and Danish formulas tend to overestimate and the Gates formula tends to underestimate PBC. Modified formulas incorporating dynamic load test values show improved accuracy but remain less precise than AI models. DNN achieved the highest overall performance, with XGB also outperforming all driving formulas. Among the formulas, the modified Hiley formula showed the greatest improvement, approaching AI model performance in some cases. For Restrike, similar trends were observed, but prediction variability increased, especially for large-diameter piles. AI models maintained higher accuracy than both original and modified formulas, though DNN's performance declined compared to EOID, with XGB and KNR occasionally showing lower percentage errors. As shown in Table 3, traditional formulas performed poorly in Restrike, and even modified versions failed to achieve substantial accuracy gains. The increased complexity of Restrike PBC—driven by grout curing and greater skin friction contributions—appears difficult to capture using driving formulas alone. AI models showed slightly reduced effectiveness in Restrike compared to EOID, they consistently provided more reliable predictions than dynamic driving formulas, highlighting their suitability for PPP PBC estimation.

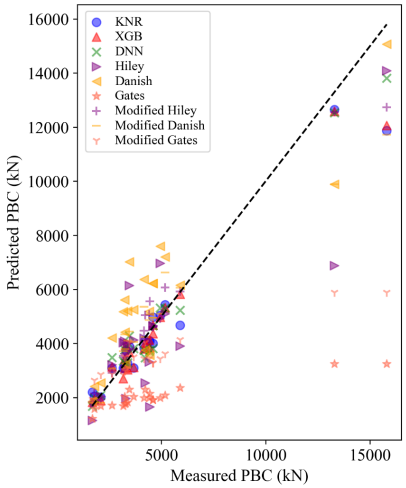

(a) EOID phase

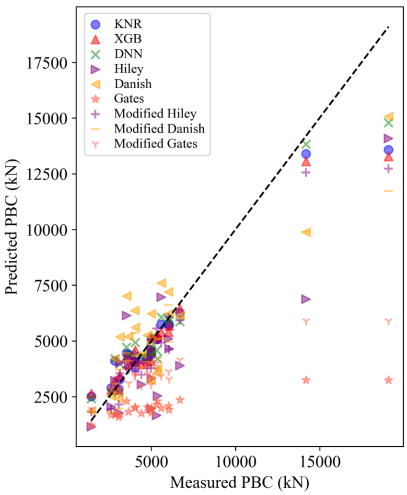

(b) Restrike phase

Figure 3. Comparison of prediction results using AI models and dynamic driving formulas for test dataset

Table 3. Prediction performance of AI models and driving formulas

Driving phase	Model	R2	MAPE	RMSE	MAE
EOID	KNR	0.919	0.102	944.888	518.865
	XGB	0.931	0.090	871.545	458.265
	DNN	0.960	0.106	661.189	489.680
	Hiley	0.685	0.241	1856.332	1188.433
	Danish	0.720	0.362	1751.686	1453.178
	Gates	-0.410	0.478	3929.314	2661.069
	Modified Hiley	0.941	0.102	803.880	491.340
	Modified Danish	0.849	0.152	1286.610	803.516
	Modified Gates	0.300	0.226	2768.126	1439.086
Restrike	KNR	0.884	0.138	1298.876	681.832
	XGB	0.874	0.134	1354.741	700.950
	DNN	0.911	0.165	1142.400	748.706
	Hiley	0.574	0.301	2491.791	1766.840
	Danish	0.750	0.301	1911.036	1489.680
	Gates	-0.613	0.551	4849.987	3451.341
	Modified Hiley	0.838	0.141	1537.603	854.390

	Modified Danish	0.731	0.187	1981.559	1153.298
	Modified Gates	0.106	0.289	3610.944	2084.731

4.3 *Comparison of prediction models suing DRF indicators*

The dynamic reduction function (DRF), derived from CAPWAP analysis of dynamic load tests, represents the ratio between measured and predicted bearing capacities and serves as a key indicator for managing working piles. Figure 4 shows DRF distributions for AI models and both original and modified driving formulas, with a DRF of 1 indicating perfect agreement with measurements. AI models (KNR, XGB, DNN) exhibited average DRF values close to 1, reflecting strong alignment with CAPWAP results. In contrast, original driving formulas showed larger deviations, while modified formulas—particularly the Modified Hiley and Danish—demonstrated improved accuracy, with DRF values generally within 1. This improvement stems from incorporating EMX values from dynamic load tests into the hammer energy calculations. Although driving formulas simplify the complex energy transfer mechanics in pile driving and require a damping factor to match test results, AI models inherently produce DRFs near 1, suggesting that DRF adjustments may be unnecessary for AI-based approaches. These findings emphasize the potential of data-driven methods to deliver accurate, reliable, and cost-effective solutions for pile capacity prediction and design.

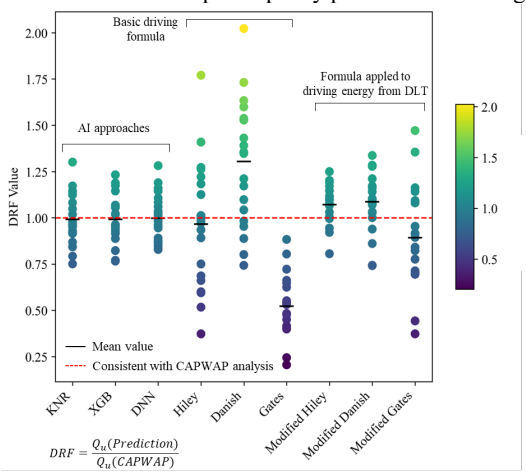

Figure 4. Results of dynamic reduction function (DRF) index for prediction models

5 CONCLUSIONS

This study evaluated AI-based models—KNR, XGB, and DNN—for predicting the pile bearing capacity of prebored and precast PHC piles across the two critical construction phases: EOID and Restrike. Direct comparison with conventional dynamic driving formulas (Hiley, Danish, Gates) demonstrated that AI models consistently achieved higher accuracy, stronger generalization, and greater robustness under varying site conditions. The DNN model, in particular, delivered the highest predictive performance, with R^2 values of 0.960 for EOID and 0.915 for Restrike, effectively capturing complex nonlinear pile–soil interactions. Unlike traditional formulas, which frequently over- or underestimate capacity due to factors such as energy transfer ratio (ETR) and set values, AI models provided stable predictions without reliance on empirical correction factors like the dynamic reduction factor (DRF). SHAP-based interpretability further revealed the dominant influence of pile diameter, ram force, and set value on PBC, offering valuable insights for practical decision-making. The results confirm that AI-driven prediction frameworks, especially when tailored for PPPs, enable phase-specific quality control, enhance construction reliability, and streamline assessment processes using readily obtainable field data. While performance in Restrike conditions showed greater variability, AI models still outperformed driving formulas, highlighting their adaptability to time-dependent effects and site-specific complexities. This research establishes AI models—particularly DNN—as a practical and reliable alternative to traditional PBC estimation methods for PPP, supporting their integration into pile testing and quality assurance workflows. Future work will focus on incorporating additional geotechnical parameters, such as soil classification and SPT-N values, to further improve accuracy and model generalization.

6 ACKNOWLEDGEMENTS

Research for this paper was carried out under the KICT Research Program (project no. 20250285-001, Development of infrastructure disaster prevention technology based on satellites SAR) funded by the Ministry of Science and ICT.

7 REFERENCES

Allin, R., Likins, G., & Honeycutt, J., 2015. Pile Driving Formulas Revisited. *In Proceedings of the International Foundations Congress and Equipment Expo 2015*, San Antonio, 1-12.

Chen, R. B., Zhang, J. C., Chen, Z. Y., & Zhang, X., 2022. New mechanical model for evaluating bearing capacity of prestressed pipe piles in soil: Effect of soil layer. *J. Test. Eval.* 50 (3), 1-16.

Denes, D., & Kroenert, B. 2019. A case study of pile testing and verification. Berth 4 upgrade – port of Townsville, *Australasian Coasts & Ports 2019 Conference*, Hobart, 1-7.

Fragaszy, R.J., Argo, D., & Higgins, J.D., 1986. Comparison of formula predictions with pile load tests. *Transportation Research Record.* 1219, 1-12.

Hazbeh, O., Rajabi, M., Tabasi, S., Lajmorak, S., Ghorbani, H., Radwan, A.E., Alvar, M.A., & Molaei, O., 2024. Determination and investigation of shear wave velocity based on one deep/machine learning technique. *Alexandria Engineering Journal.* 92, 358-369.

Heins, E., & Grabe, J., 2019. FE-based identification of pile–soil interactions from dynamic load tests to predict the axial bearing capacity. *Acta Geotechnica.* 14, 1821-1841.

Jung, G., Kim, D., Lee, C., & Jeong, S., 2017. Analysis of skin friction behavior in prebored and precast piles based on field loading test. *Journal of the Korean Geotechnical Society.* 33, 31-38.

Kim, D., Jeong S., & Park, J., 2020. Analysis on shaft resistance of the steel pipe prebored and precast piles based on field load-transfer curves and finite element method. *Soils and Foundation.* 60, 478-495.

Kordjazi, A., Nejad, F.P., & Jaksa, M. 2014. Prediction of ultimate axial load-carrying capacity of piles using a support vector machine based on CPT data, *Computers and Geotechnics.* 55. 91-102.

Lawton, E. C., Fragaszy, R. J., Higgins, J. D., Kilian, A. P., & Peters,A. J., 1986. Review of methods for estimating pile capacity. *Transportation Research Record.* 1105, Washington,D.C., 32-40.

Li, C., & Li, X., 2023. Evaluation of bearing capacity of PHC pipe piles via the dynamic and static loading test. *Frontiers in Earth Science.* 11:1130294.

Li, H., Li, S., & Ghorbani, H., 2024. Data-driven novel deep learning applications for the prediction of rainfall using meteorological data. *Frontiers in Environmental Science.* 12:1445967.

Seo, S., Chung, M., Kim, J.H., & Choi, C., 2023. Practical method for pile construction management using non-contact pile penetration movement measuring device and pile driving formulas: A case study. *Smart Geotechnics for Smart Societies: Proceedings of the 17th Asian Regional Conference on Soil Mechanics and Geotechnical Engineering*, Astana, 2117-2123.

Zhou, J.J., Yu, J.L., Gong, X.N., & Yan, T.L., 2020. Field tests on behavior of pre-bored grouted planted pile and bored pile embedded in deep soft clay. *Soils and Foundation.* 60 (2), 551-561.